COVER SHEET

Paper Number: **607**

Title: **Validation of material models for inter and intra-laminar damage in laminated composites**

Authors: Michael Bruyneel
Jean-Pierre Delsemme
Anne-Charlotte Goupil
Philippe Jetteur
Cédric Lequesne
Tadashi Naito
Yuta Urushiyama

ASC 29th Technical Conference, 16th US-Japan Conference on Composite Materials, & ASTM D30 50th Anniversary meeting UC San Diego, La Jolla, CA
Sept. 8-10, 2014, Price center, University of California San Diego, La Jolla, CA USA

ABSTRACT

In order to propose predictive finite element simulation tools, it is important to use material models able to represent the different modes of degradation of the plies forming the laminated composite structure. Damage at the interface between the plies, that is delamination, must also be taken into account.

In this paper, we present the solution available in the LMS Samtech Samcef finite element code, for the progressive damage analysis of polymer matrix laminated composites made of UD plies. The material damage models for the interfaces and the plies are described, together with the parameter identification procedure at the coupon level. Comparison between simulation and tests results validate the approach.

It is also demonstrated that, in general applications, modeling delamination alone is not enough, and it is essential to model the damage inside the plies besides the damage at the interfaces.

INTRODUCTION

Even if lots of models and methodologies are available in the literature for composite damage modelling, some of them considering delamination (inter-laminar damage) [1-6] and others dealing with ply progressive failure (intra-laminar damage) [7-11], the approach used in this paper is based on the continuum damage mechanics as described in [12-15]. The laminate is made of homogenous plies, and the interfaces between the plies are also modeled. The material laws are defined at that meso-scale, that is in the plies and in the interfaces.

In this paper, the first level of the pyramid of tests of Figure 1 is addressed. At that stage, coupons are studied, and the physical tests results are used to determine the parameters of the composite damage models.

Michael Bruyneel, Jean-Pierre Delsemme, Philippe Jetteur, Cédric Lequesne, SAMTECH (A Siemens Industry Sotware Company), Liège Science Park, Angleur, Belgium.
Anne-Charlotte Goupil, ISMANS, Le Mans, France.
Yuta Urushiyama, Tadashi Naito, Honda R&D, Tochigi, Japan.

Later on in the design process, the upper stages of the pyramid are addressed, based on the information gathered at the previous stages.

For the material model used here, damage variables impacting the stiffness of each unidirectional (UD) ply are associated to the different failure modes. They represent the fiber breaking, matrix cracking and de-cohesion between fibers and matrix. This ply damage model is first presented. Then, the basics of the parameter identification procedure of such a material model are briefly explained. This procedure is based on test results at the coupon level. It is used to determine not only the elastic properties but also the value of the parameters describing the non-linear behavior of the material. The obtained values are then validated on a comparison between test and simulation on a coupon with a stacking sequence which was not used for the identification.

The cohesive elements approach is used for the modeling of the inter-laminar damage. A damage model is assigned to interface elements inserted between plies to represent their possible de-cohesion and a fracture criterion is used to decide on the inter-laminar crack propagation. Using such cohesive elements in the analysis allows estimating not only the propagation load but also predicting the crack propagation and the residual stiffness and strength during the fracture process. The inter-laminar damage model is presented together with the basics of the parameter identification procedure relying on DCB and ENF physical tests. The obtained values are then validated on a MMB test.

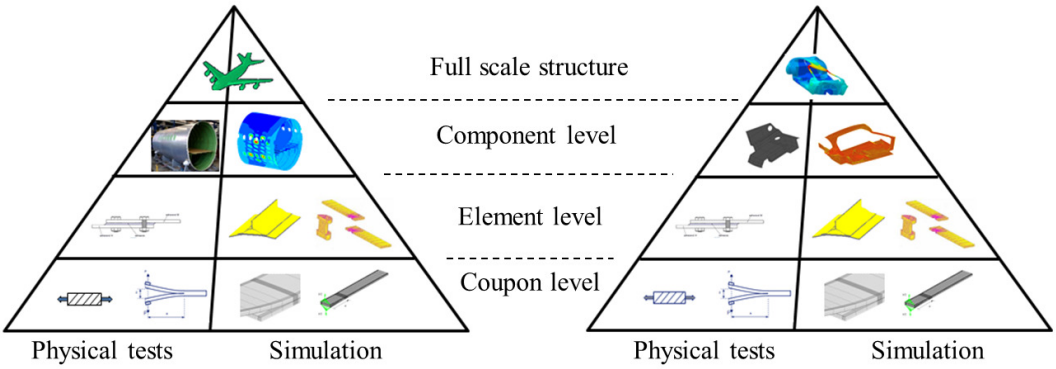

Figure 1. The pyramid of tests for composite structures, mixing physical and virtual testing, for the aerospace and automotive sectors

In this paper, it is also demonstrated that, in general applications, modeling delamination alone is not enough to get accurate results. It is essential to model damage inside the plies besides damage at the interfaces. Moreover, the importance of the permanent deformations appearing in the matrix, and so requiring the use of a plasticity law, is also discussed.

In this paper, all the computations are carried out with the LMS Samtech Samcef finite element code.

CONTINUUM DAMAGE MECHANICS

The fundamentals of continuum damage mechanics are briefly recalled here in the case of an isotropic material. Let us consider the simple Hook's law in 1D linear

elasticity (stress and strain tensors limited to σ and ε), where E^0 is the initial material stiffness (Figure 2a). The equations are written in (1), with e being the elastic potential:

$$\sigma = E^0 \varepsilon \qquad e = \frac{\sigma^2}{2E^0} \qquad \varepsilon = \frac{\partial e}{\partial \sigma} = \frac{\sigma}{E^0} \tag{1}$$

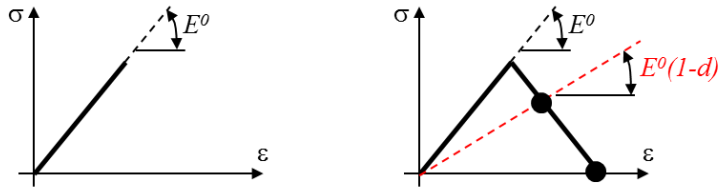

a. Linear elasticity. No damage b. Damage

Figure 2. Linear elasticity and damage: general principle

Based on Figure 2b, it is assumed that damage appears for a given limiting value of the strain. At that point, the maximum stress is reached and the mechanical properties start to decrease for an increase of the strain, as the result of a damage. As depicted in Figure 2b, the corresponding stiffness can be seen as a proportion of the initial stiffness E^0, where d is the damage variable taking its value between 0 (no damage) and 1 (completely damaged). Based on this, the potential now depends on σ and d. It then comes that:

$$\sigma = (1-d)E^0 \varepsilon \qquad e_d = \frac{\sigma^2}{2(1-d)E^0}$$

$$\varepsilon = \frac{\partial e_d}{\partial \sigma} = \frac{\sigma}{(1-d)E^0} \qquad Y = -\frac{\partial e_d}{\partial d} = \frac{\sigma^2}{2(1-d)^2 E^0} \tag{2}$$

Y is named the thermodynamic force. It is the opposite of the derivative of the potential with respect to the damage variable. It is clear that the damage will increase with the loading. In practice, damage is a function of the thermodynamic force, as illustrated in Figure 3 in a general case. Such a curve is usually obtained from tests results on coupons (as explained in the following sections of the paper).

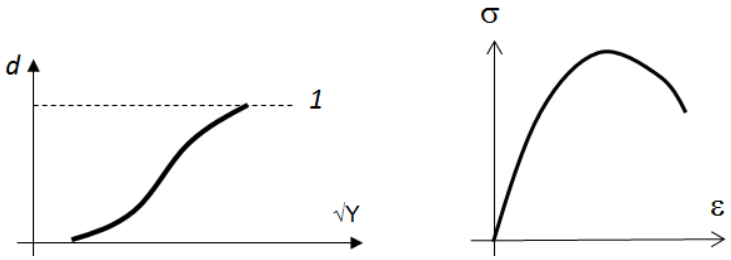

Figure 3. Damage as a function of the thermodynamic force; example of resulting constitutive law

Let's assume that the value of ε is imposed. Based on (2), Y can be expressed as a function of ε and E^0. As the relation between d and Y is known from test results (Figure 3), the stress-strain relation (constitutive law) is then completely determined. A general material behavior with non-linearity and softening is then obtained, as suggested in Figure 3.

INTRA-LAMINAR DAMAGE MODEL

Formulation of the intra-laminar damage model

Although delamination is certainly the most frequent mode of failure in laminated composites, in practical applications it is necessary to consider the ply degradation as well. Besides the classical failure criteria such as Tsai-Hill, Tsai-Wu, Hashin and Puck, an advanced intra-laminar damage model is available in Samcef. This progressive ply damage model relies on the development proposed in Ladeveze and Le Dantec [12]. The potential with damage (here in plane stress) in (3), written in the orthotropy coordinate system, is used, where d_{11}, d_{22} and d_{12} are the damages related to the fibers, the transverse and the shear directions, respectively.

$$e_d = \frac{\sigma_{11}^2}{2(1-d_{11})E_1^0} - \frac{\nu_{12}^0}{E_1^0}\sigma_{11}\sigma_{22} - \frac{\langle\sigma_{22}\rangle_+^2}{2(1-d_{22})E_2^0} + \frac{\langle\sigma_{22}\rangle_-^2}{2E_2^0} + \frac{\sigma_{12}^2}{2(1-d_{12})G_{12}^0} \qquad (3)$$

These damage variables allow considering damage associated to failure of the fibers (d_{11}), cracks in the transverse direction (d_{22}) and de-cohesion between fibers and matrix (d_{12}), as illustrated in Figure 4. The thermodynamic forces represent the effect of the loading in the corresponding mode. These thermodynamic forces are derived from the potential and manage the evolution of the damages via relations of the form $d_{11} = g_{11}(Y_{11})$, $d_{22} = g_{22}(Y_{12},Y_{22})$ and $d_{12} = g_{12}(Y_{12},Y_{22})$, as in Figure 5. For instance, the thermodynamic force associated to shear is given in (4).

$$-\frac{\partial e_d}{\partial d_{12}} = Y_{12} = \frac{\sigma_{12}^2}{2(1-d_{12})^2 G_{12}^0} \qquad (4)$$

In Figure 5, it is seen that for a laminate submitted to pure shear (σ_{12},γ_{12}), a decrease in the stiffness is observed after some loading/unloading scenarios of increased amplitude, reflecting the fact that damage occurs in the matrix. Moreover, a load release reveals the existence of permanent deformation, which is introduced via a plasticity model. On top of that, non-linearities are taken into account in the fiber direction, in traction and in compression. It is noted from equation (3) that in the transverse direction, only traction leads to damage, what is not the case for compression, assuming the unilateral action of damage in direction 2 (cracks closure in the matrix appears in compression). These behaviors result from the tests interpretation [12].

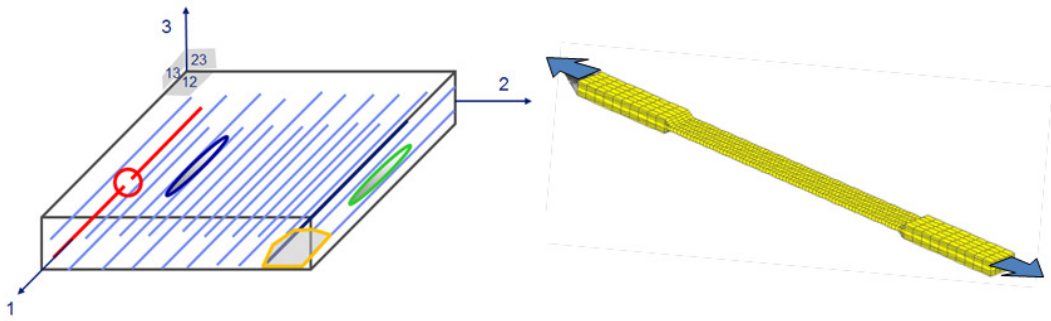

Figure 4. Possible damages in a UD ply, impacting fiber failure, matrix cracking and de-cohesion between fibers and matrix; model of the coupon

The non-linear behaviors taken into account in this model are summed up in Figure 5: they include non-linearity in the fiber direction and non-linearity including plasticity in the matrix. A delay effect can also be defined, seeing as a time regularization technique, in order to smooth the occurrence of the damages and avoid numerical issues.

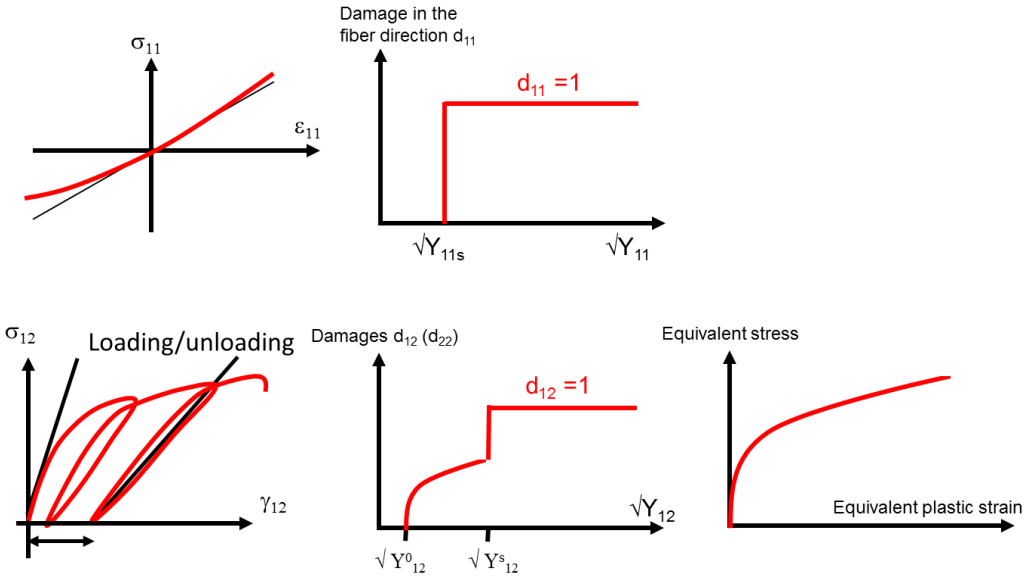

Figure 5. Non-linearities and damage evolution in the progressive damage model for UD plies

Identification procedure for the intra-laminar damage mode

From the coupon testing conducted on classical machines according to some standards like ASTM and equipped with strain gauges, the longitudinal stress σ_L and the axial and transversal strains ε_L and ε_T are obtained. Based on this information, the full (linear and non-linear) material behavior in each ply can be determined.

Four series of tests are done on coupons, each one on a specific stacking sequence and/or loading scenario. As 5 successful tests are usually required, it means that 20

tests must be conducted to cover the 4 series. This is enough to identify the parameters of the progressive damage ply model as well as the elastic properties. The identification procedure is done without extensive use of simulation. It is rather based on EXCEL sheets, and this procedure can be speed up by using some very simple FORTRAN programming. Simulation is only used to validate the identified values. The required stacking sequences mentioned above are not arbitrary; they are instead well defined, in order to be able to identify the whole set of elastic properties, as well as the value of the parameters describing the evolution of the damage and of the non-linearities of the material. For instance, one of these specific stacking sequences is made up of plies at ±45°. The loading scenario is either classical, meaning that the coupon is loaded up to the final failure, or it is based on the loading/unloading (cyclic) sequences as described in Figure 5. As an example, in Figure 6, a $[\pm 45]_{2s}$ laminate is studied. Based on the tests results as given in Figure 7, the evolution of the damage variable d_{12} is plotted as a function of the equivalent thermodynamic force Y_{12}. The hardening law of the plastic model is also identified. This allows determining the curves of Figure 5, which then feed the material model of Samcef. In Figure 7, it is checked that the results obtained with Samcef are in a very good agreement with the test results, not only for the global non-linear behavior, but also for the failure load estimation, the damage evolution (stiffness decrease measured during unloading) and the permanent deformation (plasticity). It is clear from Figure 7 that plasticity can't be neglected when studying polymer matrix composites. The hysteresis appearing during loading/unloading, which is certainly due to friction between fibers and matrix, is not taken into account in the model. Our experience is that it has no effect on the global results.

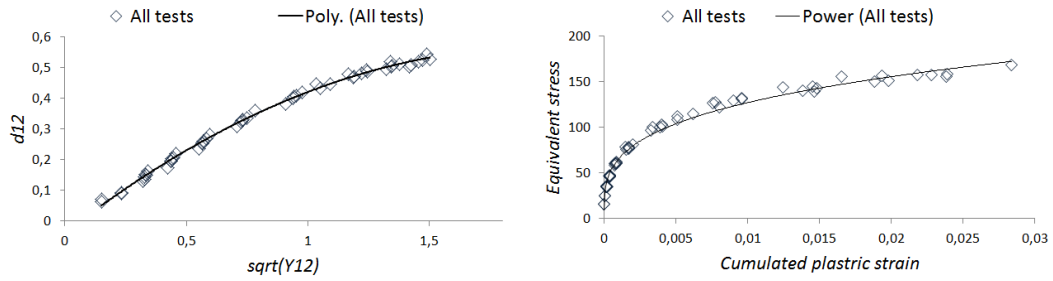

Figure 6. Non-linearities and damage evolution in the progressive damage model for UD plies

A specific angle ply laminate $[\pm\alpha_n]_s$ is considered to identify the material behavior in the transverse direction, which is actually coupled to shear. In order to take into account the coupling between shear and transverse effects, an equivalent thermodynamic force Y is used (5), and the evolution of d_{22} is, moreover, proportional to d_{12}:

$$Y = Y_{12} + bY_{22} \quad \text{and} \quad d_{22} = cd_{12} \tag{5}$$

The material behavior in the pure transverse direction is identified, as illustrated in Figure 8. The resulting damage evolutions are also given in Figure 8. This information feeds the progressive damage ply model of Samcef.

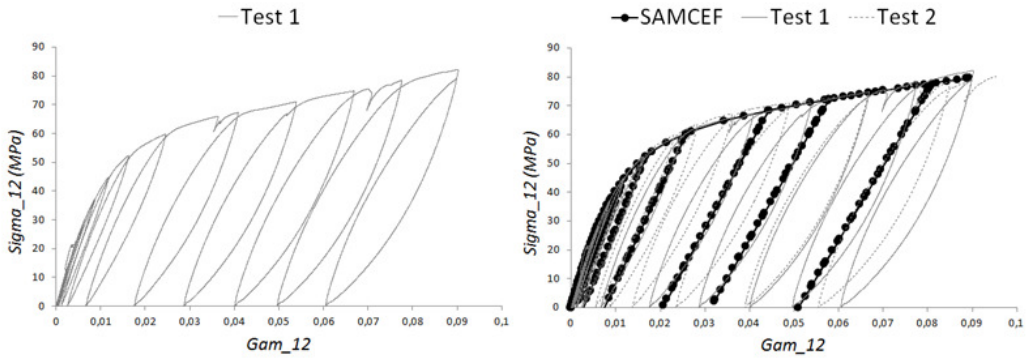

Figure 7. Non-linearities and damage evolution in the progressive damage model for UD plies. On the left, test result; on the right simulation superposed to test results

In Figure 9, the evolution of the stiffness modulus E_{11} in the fiber direction is identified, in traction (hardening effect) and compression (softening effect), as illustrated in Figure 5. The softening effect appearing in compression is (partly) due to fiber micro-buckling. The (very small) hardening effect in traction is related to the realignment of the fibers in the loading direction. The failure loads in the fiber direction are also easily determined based on the tests, in traction and in compression.

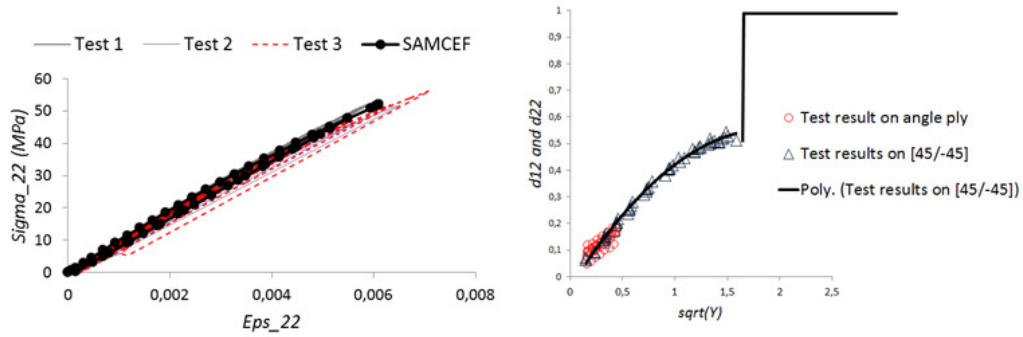

Figure 8. Identification of the material behavior in the transverse direction. Evolution of d_{12} and d_{22} as a function of the equivalent thermodynamic force Y

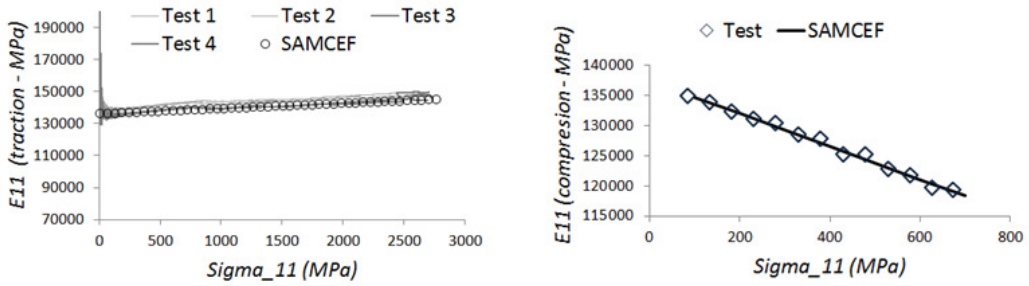

Figure 9. Evolution of E_{11} in traction and compression

In Figure 10, the longitudinal force F_L and the corresponding longitudinal strain in the coupon are plotted. This allows determining the strength in the fiber direction. In this case, the force is applied on the coupon in the model, and the displacement becomes very large when the maximum load has been reached.

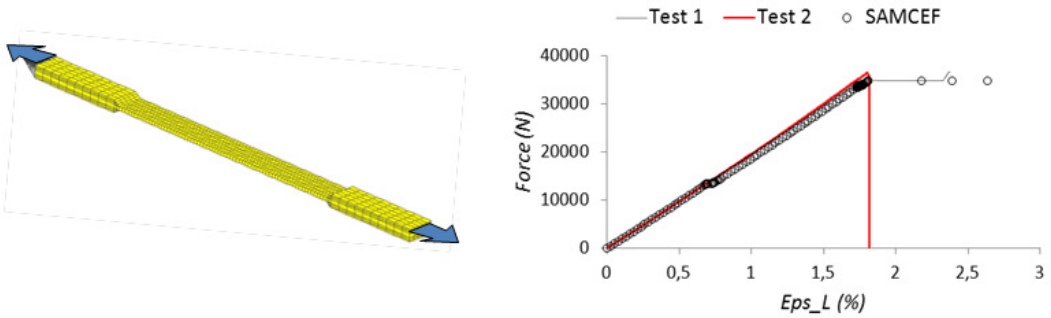

Figure 10. Load-longitudinal strain diagram for the failure in the fiber direction

From Figure 11, it is clear that when inaccurate values of the parameters are used in the progressive ply damage model, simulation results are not in a good agreement at all with the tests. In Figure 11, the damage and plasticity laws of Figure 6 were modified, as well as the strength. This solution should be compared to the one obtained in Figure 7. Comparing those two Figures, it is clear that an accurate identification procedure is necessary if one wants to be able to reproduce the non-linear behavior of the composite material.

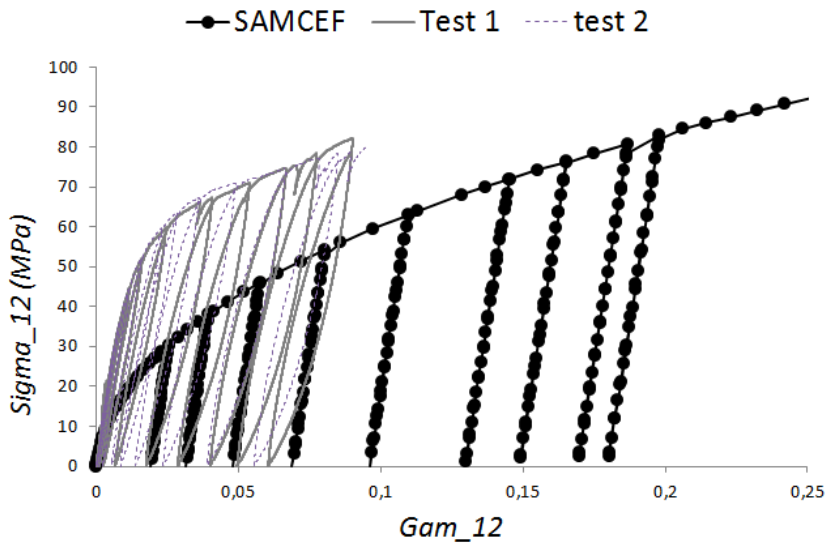

Figure 11. Comparison between tests and simulation when inaccurate values of the parameters are used

Validation

In order to validate the value of the parameters of the progressive damage model, a blind test is conducted on a $[67.5/22.5]_{2s}$ coupon. This stacking sequence was not used for the parameter identification. Simulation is run, and a comparison to test results is done. A very good agreement is obtained, as illustrated in Figure 12. Compared to the initially identified value of the parameters, just the failure load in the transverse direction had to be a little bit increased. The value of the progressive ply damage

model are then validated, and can therefore be used to study any coupon made of an arbitrary number of plies and arbitrary orientations. The only restrictions are that the base material properties (of the fibers and the matrix) and the fiber volume fraction can't be changed, and that the properties are obtained for given temperature and humidity levels. This information can also be used to predict the behavior of more complicated composite parts on the upper stages of the pyramid (Figure 1).

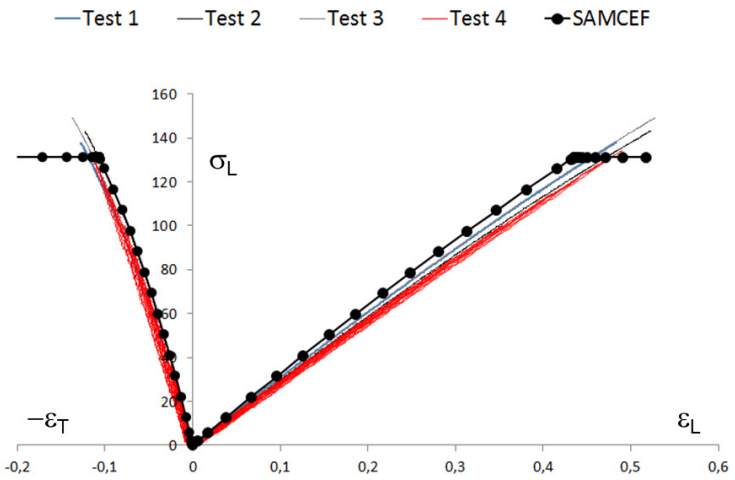

Figure 12. Validation of the values of the progressive ply damage model parameters on a $[67.5/22.5]_{2s}$ laminate

INTER-LAMINAR DAMAGE MODEL

Formulation of the inter-laminar damage model

In the approach described in [13,16], interface elements are defined between the plies in the finite element model, as depicted in Figure 13.

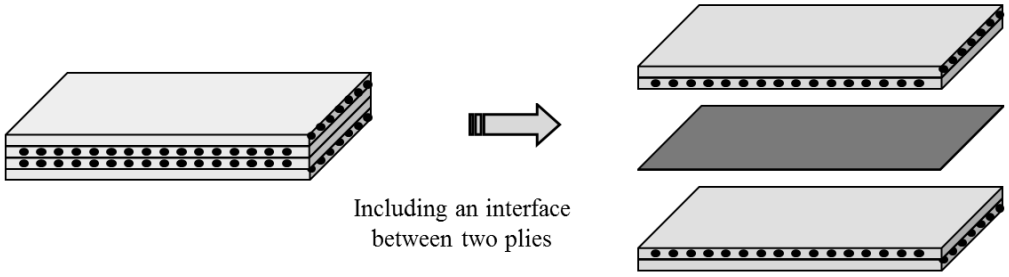

Figure 13. Interface element defined between the plies in the finite element model

The potential associated to the interface elements is given in (6), where the three relevant components of the strain tensor are considered.

$$e_d = \frac{1}{2}\left[k_I^0 \langle \varepsilon_{33} \rangle_-^2 + k_I^0 (1-d_I) \langle \varepsilon_{33} \rangle_+^2 + k_{II}^0 (1-d_{II}) \gamma_{31}^2 + k_{III}^0 (1-d_{III}) \gamma_{32}^2 \right] \quad (6)$$

k_i^0 (i=I,II,III) represent the stiffness associated to the normal strain and to the two shear effects. Damage variables d_i (i=I,II,III) are defined for each of the three crack solicitation modes as in Figure 14 (opening, shear and sliding modes, for modes I, II and III, respectively).

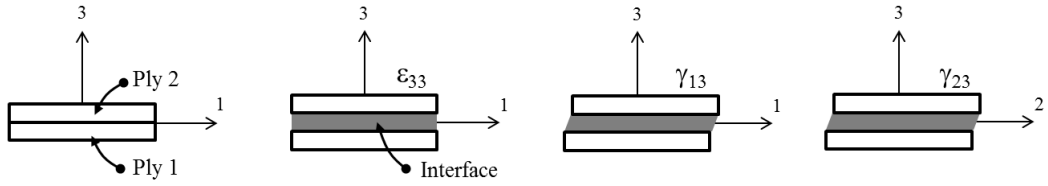

Figure 14. Definition of the interface and crack modes

The value of the damage variable $d_i \in [0,1]$ increases from 0 to 1 as a function of a thermodynamic force Y_i given by the derivative of the potential in (6) with respect to the corresponding damage variable.

$$Y_I = -\frac{\partial e_d}{\partial d_I} = k_I^0 \langle \varepsilon_{33} \rangle_+^2 \qquad Y_{II} = -\frac{\partial e_d}{\partial d_{II}} = k_{II}^0 \gamma_{31}^2 \qquad Y_{III} = -\frac{\partial e_d}{\partial d_{III}} = k_{II}^0 \gamma_{32}^2$$

The thermodynamic forces represent the effect of the loading in the corresponding mode. For mixed mode loading, the damage evolution is related to the three inter-laminar fracture toughnesses G_{Ic}, G_{IIc} and G_{IIIc}, via an equivalent thermodynamic force Y given in (7), where α is taken equal to 1. It is considered that the three damage variables have the same evolution during the loading, and a single damage variable d associated to Y is then used to represent delamination. In Samcef, depending on how d is related to Y, either a polynomial, a bi-triangular or an exponential constitutive law is used in the interface element, as illustrated in Figure 15.

$$Y = \sup_{\tau \le t} G_{IC} \left\{ \left(\frac{Y_I}{G_{IC}} \right)^\alpha + \left(\frac{Y_{II}}{G_{IIC}} \right)^\alpha + \left(\frac{Y_{III}}{G_{IIIC}} \right)^\alpha \right\}^{1/\alpha} \tag{7}$$

For the first two material models of Figure 15, damage appears after a linear elastic behavior of the interface (grey region in Figure 15), whereas this is not the case for the exponential law. Initially equal to zero, the damage variable reaches a unit value when all the resistance capacity of the interface has been consumed (G_i = G_{ic} for pure modes, or a combination of the effects via Equation 7 for mixed modes).

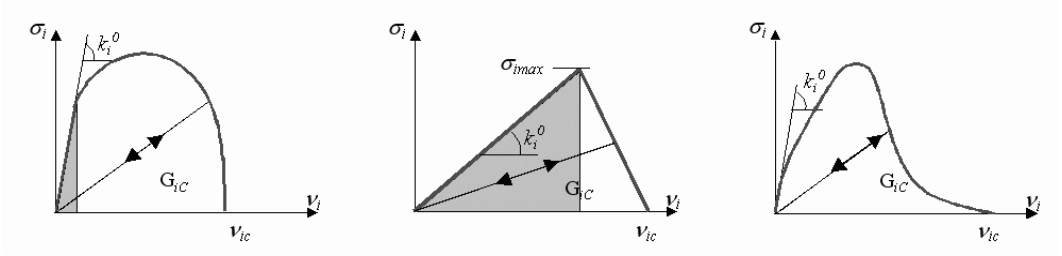

Figure 15. Cohesive laws for the interfaces

According to fracture mechanics considerations an important parameter of the model is surely the fracture toughness G_{ic}, i.e. the area under the curves of Figure 14. Contrary to fracture mechanics approaches like VCE (Virtual Crack Extension method) or VCCT (Virtual Crack Closure Technique), cohesive elements can usually be used with a coarser mesh in the crack front area [1,16]. According to [1], at least three finite elements must be active in the process zone, which is the zone where damage takes intermediate values.

Identification procedure for the inter-laminar damage mode

In this paper, the bi-triangular cohesive law of Figure 15 is used. The different parameters that must be identified are the fracture toughness G_{Ic} and G_{IIc}, assuming that $G_{IIIc} = G_{IIc}$; the initial stiffness k_I^0 and k_{II}^0, assuming that $k_{III}^0 = k_{II}^0$; the interface strengths σ_{33}^{max} and τ_{13}^{max}, assuming that $\tau_{23}^{max} = \tau_{13}^{max}$. In the material model, it is considered that the elastic energy of the interface represented by the grey triangle in Figure 15 is identical for modes I and II. It results that the inter-laminar shear strength is not independent and is given by:

$$\tau_{13}^{\max} = \sigma_{33}^{\max} \sqrt{\frac{G_{IIC} k_{II}^0}{G_{IC} k_I^0}}$$

In practice, only 0°/0° interfaces are studied, and the tested specimens are of the $[0]_n$ type. The different parameters listed previously are identified by fitting simulation to experimental results. Typically, DCB and ENF tests are conducted (Figures 16 and 17). It should be noted that the interface stiffness values are somehow artificial: that stiffness must take a high value, knowing that in a perfect interface it must be infinite. In the finite elements practice however, the smallest possible value should be preferred in order to avoid working with a too fine mesh while keeping anyway a good representation of the real physical behavior. Typical solid finite element models for DCB and ENF are illustrated in Figure 18.

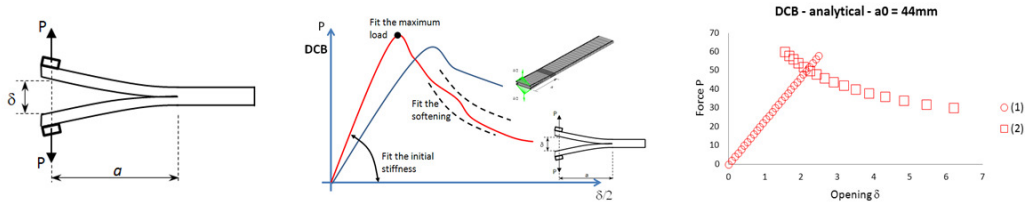

Figure 16. DCB, fitting scheme and analytical solution for a unidirectional laminate

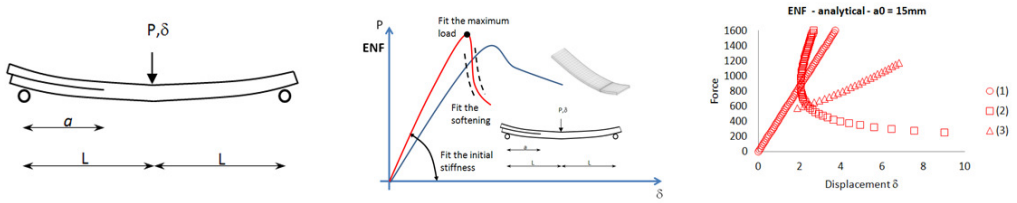

Figure 17. ENF, fitting scheme and analytical solution for a unidirectional laminate

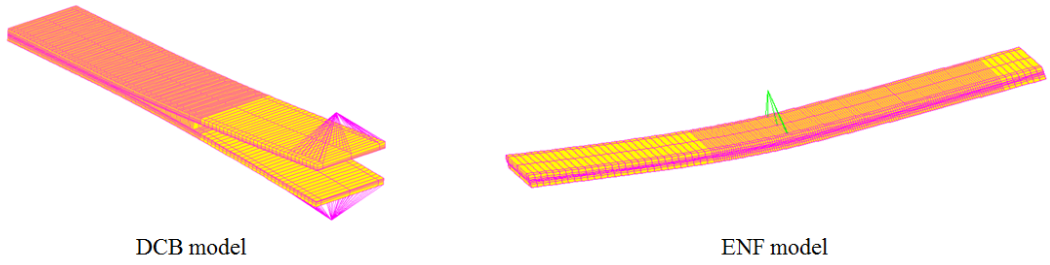

Figure 18. DCB and ENF finite element models

In Figure 19, the simulation results obtained with Samcef are compared to the physical tests on coupons. A $[0]_{16}$ laminate made up of UD plies is considered. The test results are given by the thin lines, while the analytical solution based on the beam theory is illustrated by the red circles. Samcef results are given by the black spots. It is noted that even the value of the fracture toughness G_{IC} and G_{IIC} from the test results are a little bit modified in order to perfectly fit the part of the reaction-displacement curve corresponding to the crack propagation.

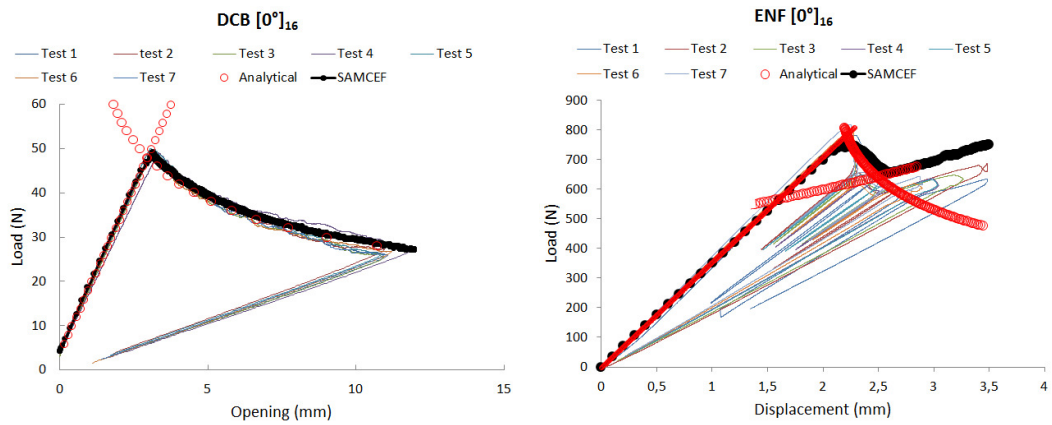

Figure 19. DCB and ENF: comparison between simulation and tests results

Validation for $[0]_n$ laminates

Usually the MMB test is used to identify the coupling between mode I and mode II. Here, we assume that $\alpha=1$, and MMB allows to validate the value of the parameters identified based on DCB and ENF as explained previously in Figures 16

and 17. The comparison between simulation and tests for MMB is given in Figure 20 for the 0°/0° interface. The good agreement between tests and simulation validates the value of the parameters. It should be noted that the initial slope of the force-displacement curve in Figure 20 depends on the initial crack length, which is sometimes difficult to measure on the coupon, what explains the small difference between simulation and tests. The part of the curves associated to the crack propagation is, however, in a good agreement.

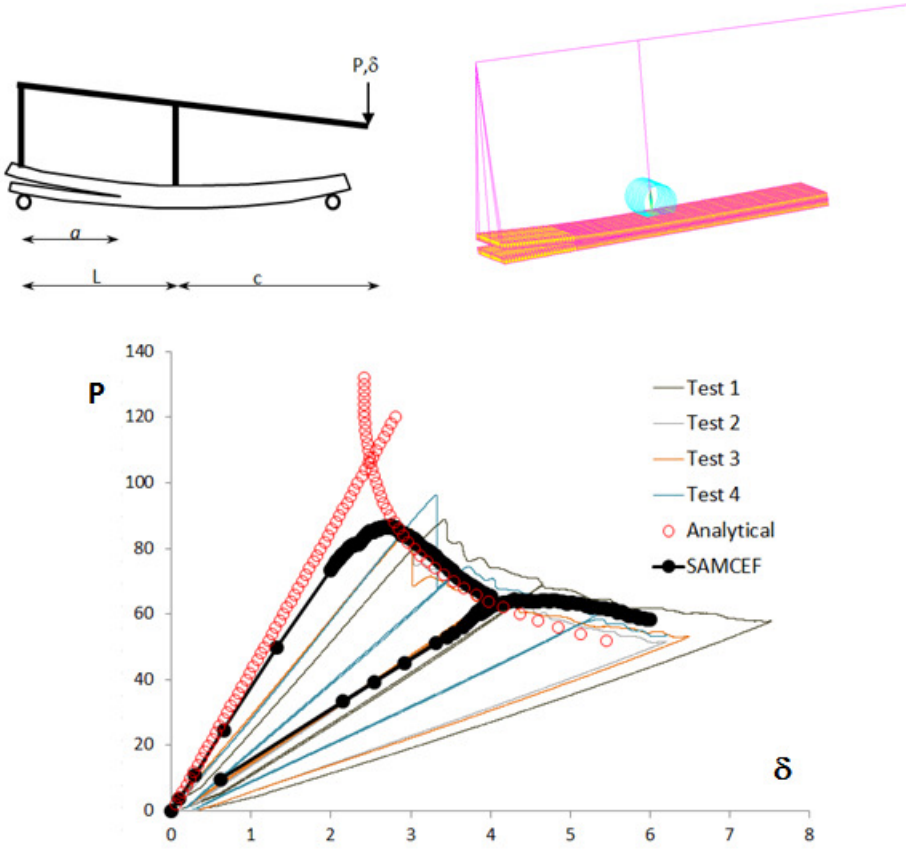

Figure 20. MMB: comparison between Samcef and tests results

USING INTER AND INTRA-LAMINAR DAMAGE MODELS

Besides the identification and validation conducted for 0°/0° interfaces as described in Figures 16 to 20, θ°/-θ° interfaces are also studied in order to show that, in a general case, it is important to model not only the damage at the interface of the plies, but also the damage inside the plies. This is illustrated for the ENF test case, as depicted in Figure 21, where simulation is compared to analytical solutions and to test results. It was observed in Figure 19 that for a $[0]_n$ laminate the behavior is quasi-linear up to the crack propagation load, which is the maximum point of the force-displacement curve. However, when the laminate includes ±45° orientations, the non-linear behavior observed in the tests can only be reproduced if the damage inside the plies is also modeled. Doing so, we note a very good agreement between

tests (light lines) and simulation (dark spots) in Figure 21; the red circles correspond to the analytical solution for delamination only. Note that for DCB and a similar stacking sequence, damage inside the ply is not observed.

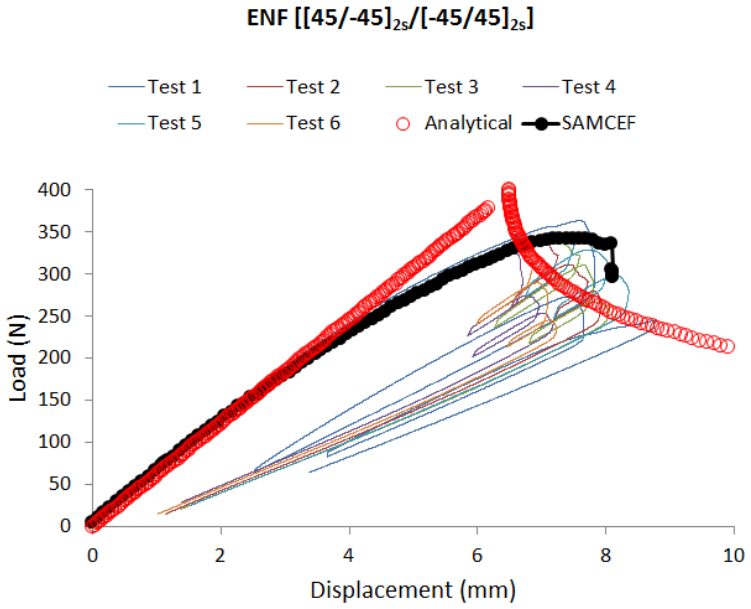

Figure 21. DCB and ENF for θ°/-θ° interfaces

CONCLUSIONS

In this paper, the solution available in the LMS Samtech Samcef finite element code for studying the progressive damage of polymer matrix laminated composites was presented. The material damage models for the interfaces and the plies were described. The formulation is based on the continuum damage mechanics. For delamination, the cohesive elements approach is used. The parameter identification procedures at the coupon level were described. It was explained that for intra-laminar damage, only 4 series of tests must be conducted at the coupon level to identify not only the elastic and strength parameters, but also the damage and plasticity laws. For delamination, the identification procedure relies on DCB, ENF and MMB tests. The approach was validated by comparisons between simulations and tests results.

It was also demonstrated that, in general applications, modeling delamination alone is not enough, and it is therefore essential to model the damage inside the plies besides the damage at their interfaces.

REFERENCES

1. Camanho, P.P. 2006. "Finite element modeling of fracture in composites: current status and future developments", presented at the NAFEMS Seminar – Prediction and Modeling of Failure Using FEA. NAFEMS, Roskilde, Denmark, 2006.
2. Krüeger, R. 1994. "Three dimensional finite element analysis of multidirectional composite DCB, SLB and ENF specimens", ISD-Report N° 94/2, Institute for Statics and Dynamics of Aerospace Structures, University of Stuttgart.

3. Krüeger, R. 2004. "Virtual Crack Closure technique: history, approach and applications", *Applied Mechanics Reviews*, 57: 109-143.
4. Krüeger, R. 2007. An approach for assessing delamination propagation capabilities in commercial finite element codes, presented at the American Society of Composites 22nd Annual Technical Conference, University of Washington, Seattle, WA, September 17-19, 2007.
5. Orifici, A.C., Thomson, R.S., Degenhardt, R., Bisagni, C. and Bayandor, J. 2007. "Development of a finite element analysis methodology for the propagation of delaminations in composite structures", *Mechanics of Composite Materials*, 43: 9-28.
6. Xie, D. and Bigger, S.B. 2006. "Progressive crack growth analysis using interface element based on the Virtual Crack Closure Technique", *Finite Elements in Analysis and Design*, 42: 977-984.
7. Tan, S.C. and Nuismer R.J. 1989. "A theory for progressive matrix cracking in composite laminates", *J. Compos. Mater.*, 23: 1029–47.
8. Li S., Reid S.R. and Soden P.D. 1998. "A continuum damage model for transverse matrix cracking in laminated fibre-reinforced composites", *Philos Trans R Soc Lond Ser A (Math Phys Eng Sci)*, 356: 2379–412.
9. Adolfsson, E. and Gudmundson, P. 1999. "Matrix crack initiation and progression in composite laminates subjected to bending and extension", *Int. J. Solids Struct.*, 36: 3131–69.
10. Katerelos, D.T.G, Varna, J. and Galiotis, C. 2008. "Energy criterion for modeling damage evolution in cross-ply composite laminates", *Compos Sci Technol*, 68: 2318–24.
11. Mayugo, J.A., Camanho, P.P., Maimi, P. and Dávila, C.G. 2010. "Analytical modeling of transverse matrix cracking of [±h/90n] composite laminates under multiaxial loading", *Mech Adv Mater Struct*, 17: 237–45.
12. Ladeveze, P. and Le Dantec, S. 1992. "Damage modeling of the elementary ply for laminated composites", *Composites Science & Technology*, 43: 123-134.
13. Allix, O. and Ladevèze, P. 1992. "Interlaminar interface modelling for the prediction of laminate delamination", *Composite Structures*, 22: 235-242.
14. Hochard C., Aubourg P.A., Charles J.P. 2001. "Modelling of the mechanical behavior of woven fabric CFRP laminates up to failure", *Composites Science & Technology*, 61, 221-230.
15. Abisset, E. (2012). "Un mésomodèle d'endommagement des composites stratifiés pour le virtual testing: identification et validation", PhD Thesis, ENS Cachan, France.
16. Bruyneel, M., Delsemme, J.P., Jetteur, P. and Germain, F. 2009. "Modeling inter-laminar failure in composite structures: illustration on an industrial case study", *Applied Composite Materials,* 16: 149-162.
17. Allix, O. 2007. "The damage meso-model for laminates – interface identification and application to delamination", *Course on Emerging Techniques for Damage Prediction and Failure Analysis of Laminated Composite Structures*, Cépaduès Editions.